applied sciences

MDPI

Article

The Development of a Novel Aluminosilicate Catalyst Fabricated via a 3D Printing Mold for Biodiesel Production at Room Temperature

Selene Díaz-González [1], Karina Elvira Rodríguez [2] and Laura Díaz [2,*]

[1] Inorganic Chemistry Department, University of La Laguna, Avda. Astrofísico Fco. Sánchez s/n, 38200 La Laguna, Spain; sdiagonz@ull.edu.es
[2] Chemical Engineering Department, University of La Laguna, Avda. Astrofísico Fco. Sánchez s/n, 38200 La Laguna, Spain; krodrige@ull.edu.es
* Correspondence: laudiaz@ull.edu.es

Featured Application: Biodiesel production at room temperature.

Abstract: Biodiesel production has gained attention as a sustainable alternative to fossil fuels, but challenges related to catalyst recovery and energy consumption remain. In this study, a novel lithium-impregnated aluminosilicate catalyst (LiSA) was developed using a 3D-printed mold, providing precise control over its structure to optimize performance. The structured catalyst featured a cylindrical shape with multiple circular channels, enhancing fluid dynamics and reactant interaction in a fixed-bed reactor. Catalyst characterization by SEM, TGA, XRD, and ICP-MS confirmed high thermal stability and uniform pore distribution. *Jatropha curcas* oil was used as feedstock, with diethyl ether (DEE) acting as a cosolvent to improve methanol solubility and enable transesterification at room temperature. The process achieved a high fatty acid methyl ester (FAME) yield, averaging 97.1% over 508 min of continuous operation, demonstrating the catalyst's stability and sustained activity. By reducing mass transfer limitations and energy demands, this approach highlights the potential of 3D-printed catalysts to advance sustainable biodiesel production, offering a scalable and efficient pathway for green energy technologies.

Keywords: aluminosilicate; biodiesel; cosolvent; heterogeneous catalyst; 3D printing

Academic Editor: Jun Cong Ge

Received: 1 December 2024
Revised: 27 December 2024
Accepted: 21 January 2025
Published: 22 January 2025

Citation: Díaz-González, S.; Rodríguez, K.E.; Díaz, L. The Development of a Novel Aluminosilicate Catalyst Fabricated via a 3D Printing Mold for Biodiesel Production at Room Temperature. *Appl. Sci.* **2025**, *15*, 1094. https://doi.org/10.3390/app15031094

1. Introduction

Biodiesel is a renewable biofuel produced from vegetable oils, animal fats, or frying oils through a transesterification reaction. In this process, triglycerides in oils react with an alcohol (usually methanol, MeOH) in the presence of a catalyst, generating fatty acid methyl esters (FAME, biodiesel) and glycerin as by-products. It is a sustainable alternative to fossil diesel, compatible with conventional engines [1]. Despite the promise of biodiesel, several challenges remain in making its production more sustainable and economically viable, especially regarding catalyst choice and reaction conditions.

Traditional biodiesel production heavily relies on homogeneous catalysts, such as sodium hydroxide (NaOH) or potassium hydroxide (KOH). While effective under moderate conditions, these catalysts present drawbacks, including complex recovery processes, contamination of by-products, and high sensitivity to water, leading to saponification issues. Furthermore, their use necessitates extensive purification steps, increasing environmental and economic costs. To address these limitations, heterogeneous catalysis has gained

prominence. Heterogeneous catalysts, which are easily recoverable and reusable, reduce purification requirements and offer an environmentally friendly alternative [2,3].

Another critical factor in biodiesel production is the reaction temperature. Homogeneous catalysts like NaOH and KOH typically operate at around 60 °C, while heterogeneous catalysts often require even higher temperatures to achieve comparable conversion rates due to slower reaction kinetics and mass transfer limitations. Recent developments in heterogeneous catalyst design, however, have aimed to lower these temperature requirements, bringing them closer to the operating range of homogeneous catalysts [4]. A promising strategy to further reduce the reaction temperature is using cosolvents. Cosolvents, such as acetone, tetrahydrofuran (THF), and biodiesel itself, facilitate phase homogenization between oil and methanol, which accelerates the reaction by minimizing initial mass transfer limitations and enhancing methanol solubility in the oil phase. By preventing unwanted side reactions, cosolvents help achieve higher biodiesel yields while minimizing energy consumption and operational costs [5].

On the other hand, using 3D printing technology in catalyst development represents a significant innovation in biodiesel production. This technique involves creating an object from an image in a layered format, typically stored in STL (Standard Tessellation Language) format. STL files describe the geometry of the object by approximating its surface using small triangles, making them widely compatible with 3D printers and slicing software. Among the various printing techniques, Fused Deposition Modeling (FDM) is the most used due to its simplicity and low cost [6–10]. In this method, a plastic filament material is melted and deposited onto the build platform, solidifying it into the desired shape as it cools.

Three-dimensional printing provides innovative solutions to design and material structure challenges, enabling the creation of intricate geometries that optimize surface area, improve mass transfer, and enhance the accessibility of active sites. These features are critical for catalytic efficiency. Furthermore, 3D printing offers a high degree of scalability and customization, allowing for tailored catalyst designs that meet specific reactor and process requirements. This adaptability gives 3D-printed catalysts a significant edge over conventionally manufactured ones, especially in performance and reusability.

Among the limited studies on 3D printing in biodiesel catalysis, one notable example used this technology to fabricate a microstructured catalytic stirring system with high mechanical resistance and reusability [11]. This system employed a potassium-loaded amorphous aluminosilicate derived from volcanic materials like pumice. However, the study utilized a batch reactor configuration, which has inherent limitations in terms of scalability and process efficiency. Continuous systems, in contrast, are better suited for industrial applications due to their ability to improve operational throughput and maintain consistent reaction conditions.

In this study, a novel lithium-impregnated aluminosilicate catalyst (LiSA) was developed using a 3D-printed mold. The catalyst features a circular structure with strategically designed holes to optimize fluid dynamics and maximize reactant interaction. This catalyst was evaluated in a fixed-bed reactor for the continuous transesterification of non-edible oils. Additionally, diethyl ether (DEE) was employed as a cosolvent, allowing the reaction to proceed efficiently at room temperature, thus reducing the energy demands of the process. The use of DEE is particularly advantageous due to its lower tendency to form peroxides compared to other common cosolvents, such as tetrahydrofuran (THF), and its lower boiling point (34.6 °C), which facilitates easier separation and purification during downstream processing. These characteristics make DEE a safer and more energy-efficient alternative for biodiesel production. The novelty of this study lies not only in the development of a lithium-impregnated aluminosilicate catalyst using 3D-printed molds but also

in the combination of this innovative catalyst design with the use of DEE as a cosolvent to enable efficient transesterification at low temperatures. This dual innovation—both the 3D-printed catalyst and the cosolvent strategy—has not been extensively explored in the field, particularly in combination. The 3D printing approach allows for precise control over the catalyst's geometric structure, optimizing fluid dynamics and minimizing mass transfer limitations, which are often challenges in traditional methods. The use of DEE further improves the solubility of methanol in the oil phase, addressing a common issue in biodiesel production.

2. Materials and Methods

2.1. Materials

For the catalyst synthesis, the following materials were employed: pumice (Panreac, Barcelona, Spain), ethyl methyl ketone (Scharlau, Barcelona, Spain, 95%), Triton Q (Sigma-Aldrich, St. Louis, MO, USA, 80%), dibutyl phthalate (Sigma-Aldrich, 98%), Butvar B-98 (Sigma-Aldrich, 99%), and polylactic acid (PLA, Sakata Filament 850, 1.75 mm diameter), and lithium nitrate anhydrous (Fisher Scientific, Hampton, NH, USA, $\geq$98%).

For biodiesel production, the following materials were employed: methanol (Sigma-Aldrich, 99.8% purity), diethyl ether (Sigma-Aldrich, 99.7% purity), and esterified *Jatropha curcas* oil extracted from seeds (0.39 mg KOH g^{-1} oil), following methods detailed in a previous study [12].

For FAME analysis, methyl heptadecanoate (Fluka Analytical, 99.9% purity) was used as an internal standard.

2.2. Catalyst Preparation

2.2.1. Three-Dimensional Printing of Molds and Tape-Casting

The negative molds, consisting of cylindrical shapes with internal channels, as shown in Figure 1, were designed using the free online program TINKERCAD (https://www.tinkercad.com/). These designs were 3D-printed using polylactic acid (PLA) filament with 75% infill and 1 cm wall thickness on a MAKERBOT printer (Brooklyn, NY, USA).

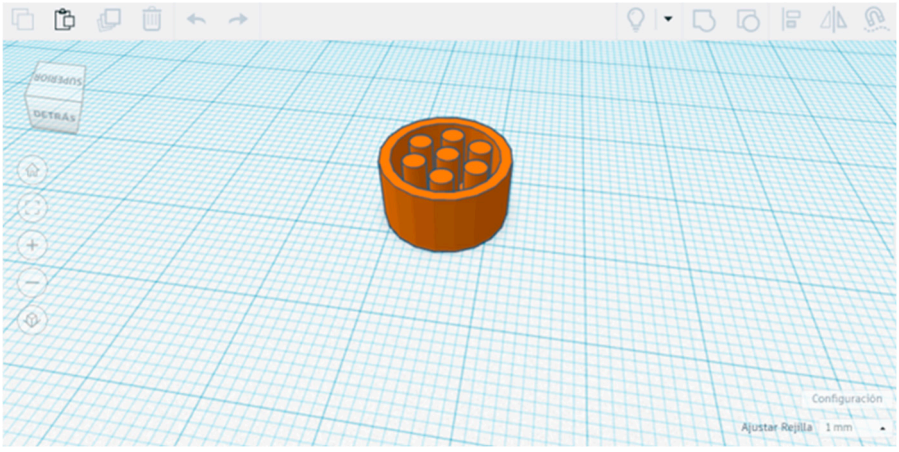

Figure 1. Negative mold design created using TINKERCAD.

A tape-casting mixture was prepared by combining pumice and ethyl methyl ketone in a 1:1 weight ratio. To this mixture, 10 wt% Butvar, 20 wt% dibutyl phthalate, and 5 wt% Triton Q (all based on the pumice weight) were added. The resulting blend was stirred for 30 min to ensure uniformity.

The molds were then filled with the prepared mixture, ensuring the complete filling of the channels and cavities. Once filled, the molds were subjected to a calcination pro-

cess in a furnace at 950 °C for 3 h, with a controlled heating ramp of 3 °C/min. During calcination, the PLA molds and organic components decomposed, leaving behind a structured pumice material with the desired cylindrical shape and internal channels. The final material, referred to as Structured Aluminosilicate Support (SAS), underwent a 20% size reduction during calcination. The resulting structure demonstrated mechanical stability and geometric precision.

2.2.2. Impregnation Method

The SAS material was impregnated with lithium nitrate to achieve a 5 wt% lithium loading. Lithium nitrate was dissolved in deionized water and added to the support (SAS). The impregnated material was dried at 100 °C for 24 h and subsequently calcined at 650 °C for 5 h. The resulting material, designated as lithium-impregnated structured aluminosilicate (LiSA), was used as a catalyst in subsequent reactions.

2.3. Catalyst Characterization

The micrographs of the SAS and LISA materials were acquired using a ZEISS (Jena, Germany) EVO 15 scanning electron microscope (SEM) with a resolution of 2 nm. To enhance conductivity and image quality, the samples were coated with a thin layer of gold using a sputtering technique prior to imaging.

The X-ray diffraction (XRD) analyses were performed using a PANalytical Empyrean diffractometer. XRD patterns were acquired using Cu Kα1 radiation (λ = 1.546 Å), with a rate scanning of 10° to 80° in terms of 2θ. Phase analysis was carried out using X'Pert HighScore Plus software (https://www.malvernpanalytical.com/es/products/category/software/x-ray-diffraction-software/highscore-with-plus-option, accessed on 30 November 2024) and the PDF-4 database.

The thermal stability of the materials was assessed using thermogravimetric analysis (TGA) on a Discovery SDT650 instrument (TA instruments, New Castle, DE, USA). Approximately 20–28 mg of the sample were placed in alumina pans with a capacity of 90 µL. Each sample was subjected to a temperature ramp from 30 °C to 1000 °C at a rate of 10 °C/min under an air atmosphere. Prior to heating, the system was equilibrated at 30 °C to ensure consistent initial conditions.

The specific surface area (S_{BET}) and average pore diameter (D) of the SAS and LiSA materials were measured using Brunauer–Emmett–Teller (BET) method, employing an ASAP 2100 porosimeter (Micromeritics Instruments Co., Norcross, GA, USA) at −196 °C. Prior to analysis, the samples were degassed at 150 °C for 12 h under vacuum.

Lithium content in the catalysts was determined by inductively coupled plasma mass spectrometry (ICP-MS) using an Agilent 7900 ICP-MS with an orthogonal detector system (ODS) (Agilent, Santa Clara, CA, USA). Prior to analysis, solid samples were subjected to a two-step microwave-assisted acid digestion. In the first stage, samples were digested with a mixture of concentrated nitric, hydrochloric, and hydrofluoric acids to dissolve the matrix. To eliminate the highly corrosive HF, a second digestion step was performed using 4% (*w*/*v*) boric acid, which effectively neutralizes HF.

2.4. Catalytic Activity and Reaction System

Biodiesel production was conducted in a fixed-bed catalytic reactor, with a length of 20 cm and an inner diameter of 1 cm, utilizing LiSA as a novel aluminosilicate catalyst fabricated via a 3D-printed mold. As shown in Figure 2, the setup included a jacketed glass reactor loaded with 40 LiSA catalyst particles, with a total approximate weight of 7.4610 g, each weighing approximately 0.1865 g. *Jatropha curcas* oil was introduced into a 1 L heated vessel equipped with a reflux condenser and mechanical stirrer and then allowed to cool to room temperature (25 °C). MeOH and DEE were pre-mixed and then added in the required

amounts based on the optimal conditions from a previous study (MeOH-to-oil molar ratio of 20:1 and DEE-to-MeOH ratio of 0.57) [13]. The mixture was stirred continuously at 400 rpm, and the feed was pumped from the vessel to the reactor at a flow rate of 1.4 mL/min. The cylindrical reactor was packed with the 3D-printed LiSA catalyst particles. Over 508 min, reaction products were collected at the reactor outlet, with 25 mL samples taken approximately every 18 min (a total of 28 samples were collected). Excess MeOH and DEE were removed by evaporation. The biodiesel product was separated from glycerol using a settling funnel, and the upper biodiesel phase was analyzed using a Varian 3900 gas chromatograph (GC-FID) to determine the FAME content, following the UNE-EN 14103:2020 standard [14].

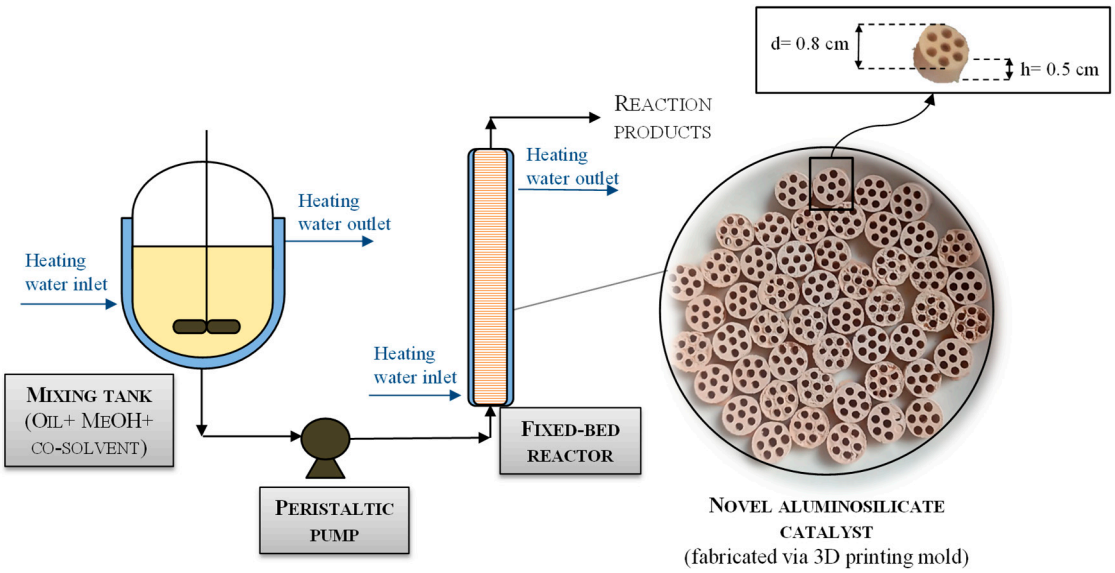

Figure 2. Setup of the fixed-bed reactor for biodiesel production using the 3D-printed aluminosilicate catalyst (LiSA).

3. Results

3.1. Catalyst Characterization

Figure 3 presents scanning electron microscopy (SEM) images of the SAS (a, b, c) and LiSA (d, e, f) materials at magnifications of 600×, 1200×, and 2000×, respectively. The SEM micrographs of SAS reveal a porous structure composed of irregularly shaped particles that form a network of interconnected voids. At higher magnifications, a rough surface texture and an intricate arrangement of particles with pronounced angular features are observed. The particle size distribution for SAS ranges approximately from 1 to 10 µm, with an estimated average size of around 5 µm. In contrast, the SEM micrographs of LiSA exhibit a distinctive morphology characterized by a more uniform distribution of smaller particles. At 1200× and 2000×, LiSA particles display a finer texture, a more homogeneous size distribution, and smoother surfaces compared to SAS. Furthermore, at 2000×, LiSA particles show a more spherical shape and a more regular pore structure. The particle size distribution for LiSA is narrower, approximately 0.5 to 3 µm, with an estimated average size of around 1.5 µm. The differences in morphology and particle size reflect the effects of the lithium impregnation process, contributing to the observed structural uniformity and reduction in particle size.

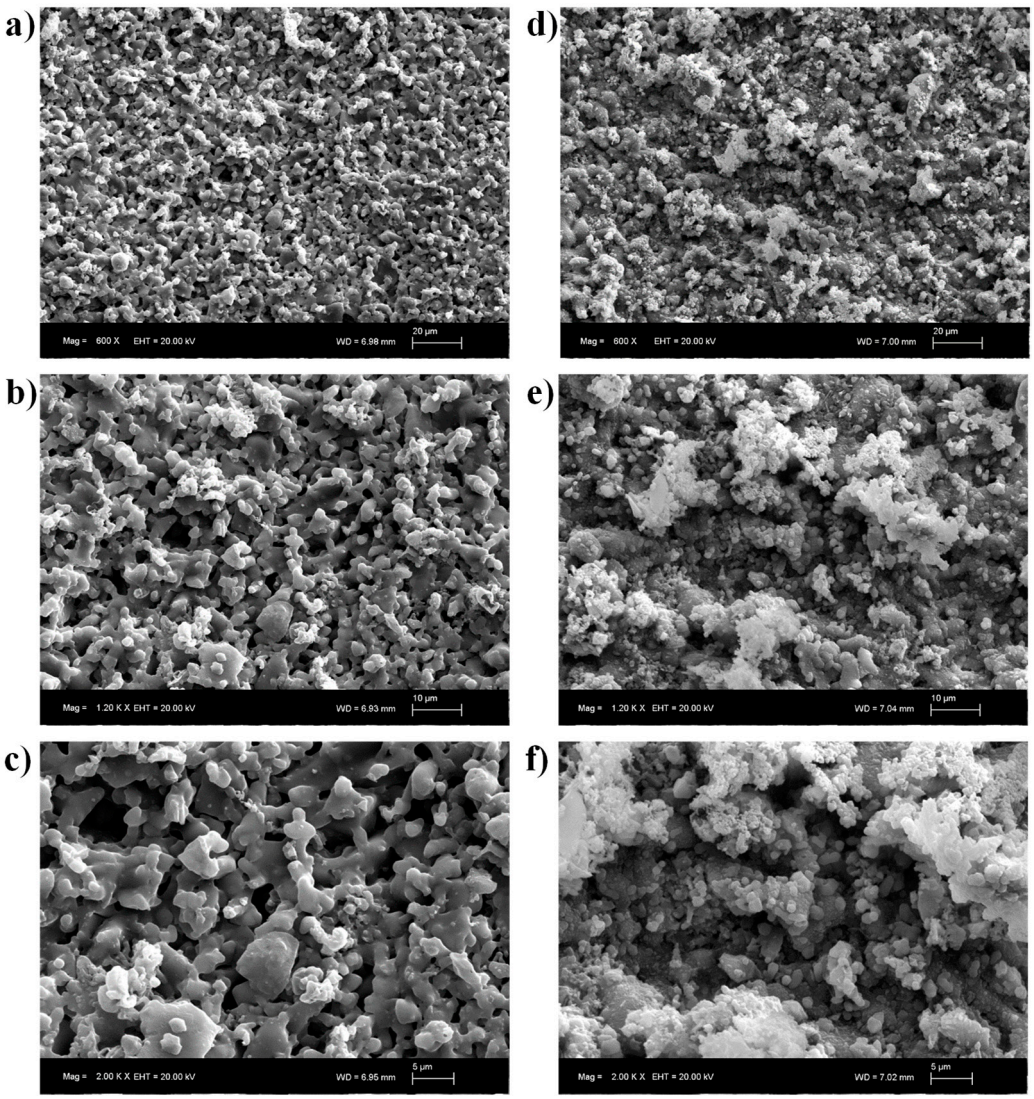

Figure 3. SEM images of SAS (**a**,**b**,**c**) and LiSA (**d**,**e**,**f**) at magnifications of 600×, 1200×, and 2000×, respectively.

Figure 4a shows the XRD patterns of the structured aluminosilicate material (SAS) and the lithium-impregnated aluminosilicate (LiSA). The diffractogram of SAS reveals an amorphous structure consistent with the pumice composition, which matches the PDF-5 ICDD database entry 00-041-1481 corresponding to $Al_{1.8}Si_{2.2}Ca_{0.8}Na_{0.2}O_8$. In the case of LiSA, the pattern exhibits a superposition of the amorphous SAS and crystalline lithium silicate (Li_2SiO_3), identified by its characteristic peaks at 18.9°, 27.0°, 33.1°, 38.6°, 43.3°, 51.8°, 55.5°, and 59.2° (space group C m C 21). This indicates the successful integration of lithium into the amorphous pumice matrix.

The thermogravimetric analysis (TGA) in Figure 4b demonstrates that both materials, SAS and LiSA, exhibit minimal weight loss, with values below 1.2% over the temperature range from 25 °C to 1000 °C. This low weight loss percentage confirms the high thermal stability of both materials. The SAS material shows a gradual weight loss, mainly below 400 °C, likely due to the desorption of physisorbed water and minor impurities within the aluminosilicate structure. After reaching 400 °C, the weight loss stabilizes, indicating the absence of significant thermal decomposition at higher temperatures. This stability suggests that the aluminosilicate support is capable of withstanding high temperatures, making it a viable candidate as a catalytic support. The LiSA material demonstrates an even lower weight loss than SAS across the entire temperature range. Initially, up to

approximately 200 °C, LiSA shows a small weight reduction, likely associated with the release of surface-adsorbed water. From 200 °C to around 500 °C, LiSA experiences a more gradual weight loss compared to SAS, possibly due to minor structural adjustments or the stabilization of lithium species within the aluminosilicate framework. Beyond 500 °C, the weight loss rate decreases significantly, showing a more stable profile up to 1000 °C. Notably, the overall weight loss in LiSA across the full temperature range is less than that of SAS, suggesting that lithium impregnation enhances the thermal stability of the support.

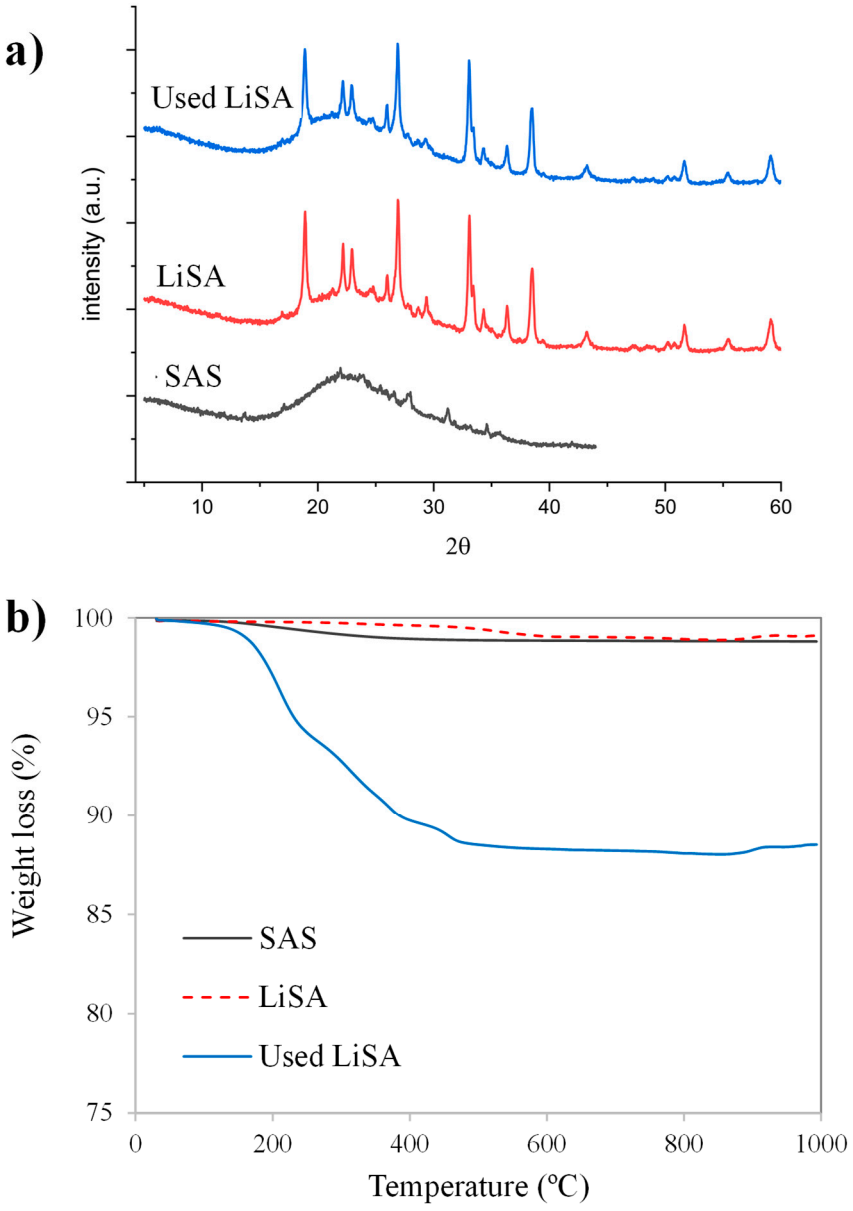

Figure 4. XRD patterns (**a**) and TGA curves (**b**) of structured aluminosilicate materials.

The specific surface area (S_{BET}) and average pore diameter (D) values obtained from nitrogen adsorption–desorption isotherms are summarized in Table 1. A decrease in the S_{BET} was observed after lithium impregnation of the support material. This reduction suggests that the support's surface becomes coated, and micropores are filled during the impregnation process. This behavior aligns with previous reports on supported materials impregnated with active metals [15].

Table 1. Surface area, average pore diameter, and lithium content of the studied materials.

Material	S_{BET} (m^2/g)	D (nm)	mg Li/g
SAS	0.62	80.3	0.0
LiSA	0.18	102.3	15.2
Used LiSA	0.16	158.7	33.5

Furthermore, the results reveal changes in the average pore diameter, indicating partial pore blockage due to lithium incorporation into the support matrix. This phenomenon, leading to a decrease in specific surface area, is consistent with trends reported in the literature for impregnated materials [16,17].

Additionally, the D values confirm that the materials exhibit a mesoporous or macroporous structure (pore diameter > 2 nm), as further corroborated by scanning electron microscopy (SEM) images (Figure 3). This structure is crucial for reducing diffusion limitations when interacting with bulky molecules like triglycerides, which are estimated to have diameters of 2–4 nm based on molecular modeling [18].

The lithium content analysis by ICP-MS (Table 1) revealed that the initially structured aluminosilicate (SAS) material contained no detectable lithium, while the impregnated material (LiSA) showed a concentration of 15.2 mg Li/g, which corresponds to 1.52% by weight of lithium. Although theoretical calculations prior to impregnation indicated an expected lithium loading of 5% by weight, the final obtained value is lower. This deviation aligns with findings reported in the literature and can be attributed to several factors inherent to the impregnation process.

Firstly, impregnation efficiency is rarely 100%, as some of the precursors may not fully interact with the support during the process. Additionally, losses during drying and calcination can occur. The drying stage is particularly critical, as it can lead to redistribution of the impregnated lithium within the support, potentially resulting in non-uniform distribution. Moreover, the structural properties of the support, such as its porosity and density, play a significant role. Denser regions at the edges of the support may retain different amounts of lithium compared to less dense areas, leading to localized variations in concentration [19]. Finally, the interaction between the lithium precursor and the aluminosilicate support influences the final lithium loading. If the interaction is weak, lithium may aggregate into larger, unsupported particles, reducing its homogeneous incorporation into the matrix [20]. Despite these variations, the lithium incorporation was confirmed by XRD patterns, supporting the successful impregnation of lithium.

3.2. Catalytic Activity

In preliminary tests conducted without using diethyl ether as a cosolvent, the immiscibility between methanol and oil created significant challenges in the reactor. At high flow rates, the reactants did not remain in contact with the catalyst long enough, resulting in low biodiesel yields. Conversely, at lower flow rates, phase separation occurred within the reactor, further hindering reactant interaction. The addition of DEE overcame these limitations by homogenizing the phases, improving fluid dynamics, and ensuring effective contact between reactants and the catalyst.

The catalytic performance of the LiSA catalyst was evaluated over a reaction period of 508 min, with reaction products collected at the reactor outlet. A total of 28 samples, each of 25 mL, were taken approximately every 18 min. The %FAME content of these biodiesel samples ranged from 94.7% to 99.6%, with an average of 97.1%, as shown in Table 2 and plotted over time in Figure 5. These results confirm the reliable long-term performance of the catalyst, demonstrating its efficiency in sustaining biodiesel production that consistently

meets commercial standards, exceeding the minimum requirement of 96.5% established by the UNE-EN 14214:2020 standard for biodiesel commercialization [21].

Table 2. %FAME content for each sample collected at the outlet of the fixed-bed reactor with LiSA catalyst.

Sample Number	t (min)	FAME (%)
1	22	97.4
2	40	97.4
3	58	98.2
4	76	99.3
5	94	99.4
6	112	98.0
7	130	98.8
8	148	97.8
9	166	97.3
10	184	96.9
11	202	96.1
12	220	96.2
13	238	95.3
14	256	94.7
15	274	94.7
16	292	94.8
17	310	95.7
18	328	95.3
19	346	96.2
20	364	96.3
21	382	96.1
22	400	98.2
23	418	98.7
24	436	98.1
25	454	99.6
26	472	97.5
27	490	97.8
28	508	97.1

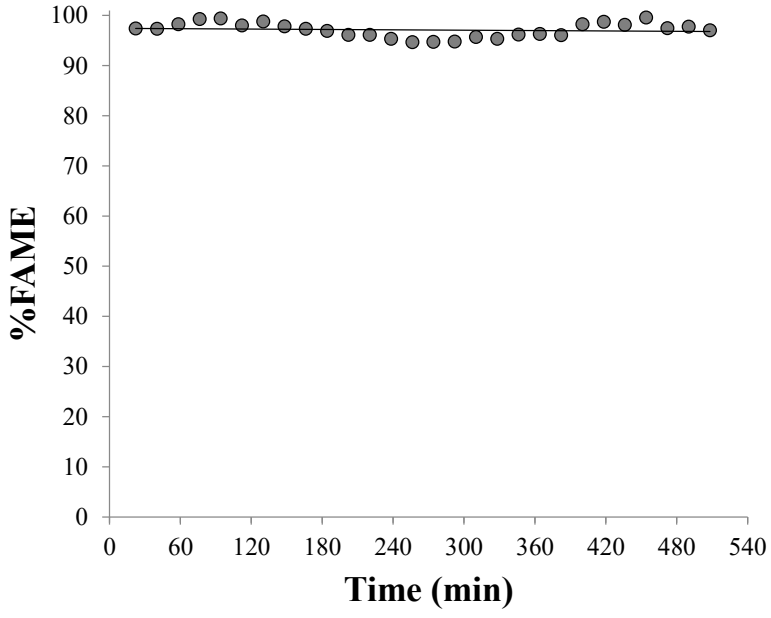

Figure 5. Evolution of %FAME content over time during transesterification reaction using the LiSA as a catalyst.

Additionally, Figure 6 displays chromatograms for two randomly selected samples: sample 12 (at 220 min), with a %FAME content of 96.2%, and sample 28 (at 508 min), with 97.1%. These chromatograms confirm the stability and reproducibility of the process over time, with only minor variations in the FAME content observed among the samples. This consistent performance highlights the high catalytic activity of the LiSA catalyst for sustained biodiesel production. Furthermore, for the two samples, a photograph of the reaction products is shown once the MeOH and DEE have evaporated. The upper phase, containing the FAME (biodiesel phase), and the lower phase, consisting of glycerol, can be observed.

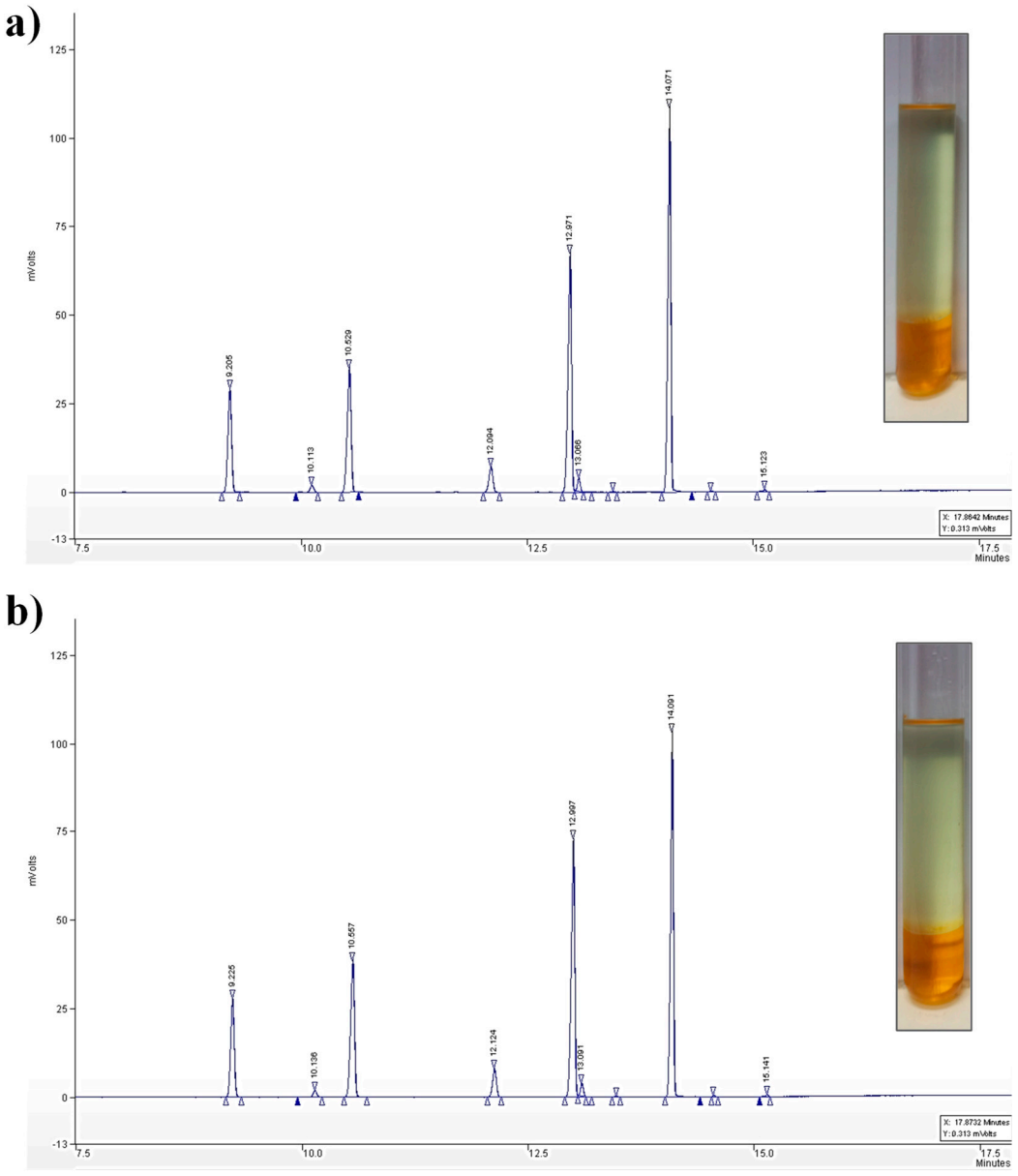

Figure 6. Chromatograms of (**a**) sample 12 at 220 min (%FAME 96.2%) and (**b**) sample 28 at 508 min (%FAME 97.1%).

Although no studies have currently been found on the development of molds for the synthesis of catalysts for biodiesel production in a fixed-bed reactor, there are some studies that, although not using 3D synthesis methods or fixed-bed reactors, do use catalysts impregnated with lithium for biodiesel production in batch processes. Among these studies, it is worth mentioning that Wen et al. [22] used Kalsilite as a heterogeneous catalyst for

biodiesel production from soybean oil and methanol. Kalsilite exhibited low catalytic activity, but by introducing 2.3% by weight of Li (using lithium nitrate as a precursor) via the impregnation method, the activity was significantly enhanced. Specifically, a 100% FAME yield was achieved at a reaction temperature of 120 °C. On the other hand, Salim et al. [23] used lithium–zeolite as a catalyst for biodiesel production from non-edible castor oil. A maximum FAME yield of 92% was reached at 60 °C, 1 h, with a 6:1 MeOH/oil molar ratio and a catalyst load of 1.5%.

In contrast to studies that operate at elevated temperatures, the present study works at room temperature, which offers a significant advantage in terms of energy efficiency. Although a cosolvent is used in this process, specifically DEE, it evaporates along with the methanol and can be reused. DEE, with a boiling point of 34.6 °C, has shown potential to improve the solubility of methanol (boiling point 64.7 °C) in the oil phase, thereby enhancing the reaction efficiency at lower temperatures. Despite environmental considerations associated with DEE, its primary advantage lies in its ease of recovery and reuse, making it a practical option for systems where temperature reduction is desirable. This use of a cosolvent in biodiesel production not only eliminates the need for external heating, thus reducing energy consumption but also aligns with the goals of sustainable and cost-effective biodiesel synthesis. Additionally, the LiSA catalyst, synthesized using a 3D-printed mold, offers the flexibility to design the catalyst with the desired shape. Due to its robust structure, it can be effectively employed in continuous biodiesel production by packing it into fixed-bed reactors. This presents a significant advantage in the biofuels industry, as continuous processes are generally more efficient and scalable compared to batch-stirred reactors, which can pose operational challenges for continuous production.

3.3. Stability of the LiSA Catalyst

To evaluate the stability of the LiSA catalyst, SEM, XRD, TGA, and lithium content analyses were conducted after 508 min of use. Figure 4a,b compare the diffractograms and TGA curves of fresh and used LiSA catalysts, showing that the crystallinity of the catalyst remained largely unaffected by the reaction. However, TGA revealed a 12% weight loss between 100 °C and 180 °C, indicating the presence of residual organic matter. These findings are consistent with the SEM images (Figure 7b), which further illustrate the presence of surface deposits of reaction products on the catalyst after 508 min of operation. Despite these observations, no significant decline in catalytic activity was noted throughout the reaction period, as evidenced by the %FAME values remaining above commercial standards (Figure 5).

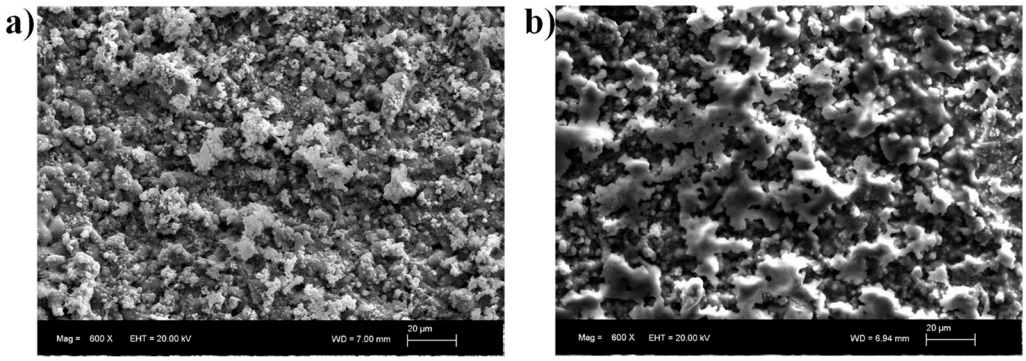

Figure 7. SEM images of the LiSA catalyst: (**a**) fresh catalyst, and (**b**) used catalyst after 508 min of reaction.

The sustained catalytic performance of the LiSA catalyst may be attributed to the absence of lithium leaching during the reaction. ICP analysis revealed not a decrease but

an apparent increase in lithium content after the reaction (Table 1). While lithium levels are not expected to rise, as the oil feedstock does not contain lithium, this anomaly might be explained by the previously discussed non-homogeneous lithium distribution within the support matrix. It is plausible that lithium remains intact and does not diminish during the reaction, but its uneven distribution may lead to localized variations in concentration, giving the impression of an increase.

This combination of structural stability and resistance to lithium leaching underscores the robustness of the LiSA catalyst, making it a promising candidate for prolonged biodiesel production processes.

This study highlights the advantages of utilizing a structured lithium-impregnated aluminosilicate (LiSA) catalyst synthesized with innovative 3D-printed molds, demonstrating enhanced catalytic activity, stability, and thermal robustness for biodiesel production under room temperature conditions. The findings underscore the energy efficiency of the process, attributed to the cosolvent-assisted transesterification and the potential for cosolvent recovery and reuse. Moreover, the adaptability of the 3D-printed catalyst shape to continuous fixed-bed reactor systems presents a scalable and sustainable solution for industrial biodiesel production. Future work should explore the long-term operational stability of the LiSA catalyst under industrial conditions and evaluate alternative, more sustainable cosolvents to further minimize environmental impacts. For example, solvents such as ethanol, a renewable and biodegradable cosolvent, could offer environmental benefits over conventional synthetic options. Additionally, glycerol, a byproduct of biodiesel production, may be an effective cosolvent, reducing waste and enhancing process sustainability. Propylene glycol and certain vegetable-derived fatty acids could also be explored for their biodegradability and lower toxicity.

4. Conclusions

The results obtained in this study confirm the viability of the LiSA catalyst for biodiesel synthesis under mild operating conditions, achieving a high %FAME content with an average of 97% maintained over 508 min of reaction, exceeding the requirements set by the UNE-EN 14214 standard. The LiSA catalyst demonstrated excellent thermal stability and structural integrity, as confirmed through comprehensive characterization. The combination of 3D printing and lithium impregnation provides a versatile and scalable method for catalyst preparation, aligning with industrial demands for continuous processes. This research not only advances the field of heterogeneous catalysis for biofuel production but also sets the foundation for the development of energy-efficient and environmentally friendly transesterification processes. Future investigations should focus on scaling up the technology, assessing the economic and environmental benefits in real-world applications, and exploring the catalyst's long-term reusability and performance under diverse feedstock conditions.

Author Contributions: Conceptualization, S.D.-G., K.E.R. and L.D.; methodology, S.D.-G., K.E.R. and L.D.; software, S.D.-G. and K.E.R.; validation, L.D.; formal analysis, S.D.-G. and L.D.; investigation, S.D.-G., K.E.R. and L.D.; resources, L.D.; data curation, S.D.-G. and L.D.; writing—original draft preparation, S.D.-G. and L.D.; writing—review and editing, S.D.-G., K.E.R. and L.D.; supervision, L.D.; project administration, L.D. All authors have read and agreed to the published version of the manuscript.

Funding: This research received no external funding.

Institutional Review Board Statement: Not applicable.

Informed Consent Statement: Not applicable.

Data Availability Statement: The original contributions presented in the study are included in the article; further inquiries can be directed to the corresponding author.

Acknowledgments: The authors would also like to acknowledge the General Service Research Support of the Universidad de La Laguna for their instrumental and technical support.

Conflicts of Interest: The authors declare no conflicts of interest.

References

1. Ray, A.; Bhonsle, A.K.; Singh, J.; Trivedi, J.; Atray, N. Examining Alternative Carbon Resources for Sustainable Energy Generation: A Comprehensive Review. *Next Energy* **2025**, *6*, 100194. [CrossRef]
2. Oyekunle, D.T.; Barasa, M.; Gendy, E.A.; Tiong, S.K. Heterogeneous Catalytic Transesterification for Biodiesel Production: Feedstock Properties, Catalysts and Process Parameters. *Process Saf. Environ. Prot.* **2023**, *177*, 844–867. [CrossRef]
3. Sarangi, P.K.; Singh, A.K.; Ganachari, S.V.; Pengadeth, D.; Mohanakrishna, G.; Aminabhavi, T.M. Biobased Heterogeneous Renewable Catalysts: Production Technologies, Innovations, Biodiesel Applications and Circular Bioeconomy. *Environ. Res.* **2024**, *261*, 119745. [CrossRef] [PubMed]
4. Parameshwar, S.; Agnihotri, M.; Bhan, U.; Nangan, S.; Verma, D.; Rajendran, S.; Jain, S. Developments in the Utilization of Heterogeneous Catalysts for Biodiesel Generation: An Update on Recent Advancements. *J. Taiwan Inst. Chem. Eng.* **2024**, 105810. [CrossRef]
5. Díaz, L.; Horstmann, F.; Brito, A.; González, L.A. A Comprehensive Review of the Influence of Co-Solvents on the Catalysed Methanolysis Process to Obtain Biodiesel. *Heliyon* **2023**, *9*, e13006. [CrossRef]
6. Nadagouda, M.N.; Ginn, M.; Rastogi, V. A Review of 3D Printing Techniques for Environmental Applications. *Curr. Opin. Chem. Eng.* **2020**, *28*, 173–178. [CrossRef]
7. Zastrow, M. 3D Printing Gets Bigger, Faster and Stronger. *Nature* **2020**, *578*, 20–23. [CrossRef]
8. Karakurt, I.; Lin, L. 3D Printing Technologies: Techniques, Materials, and Post-Processing. *Curr. Opin. Chem. Eng.* **2020**, *28*, 134–143. [CrossRef]
9. Patel, R.; Desai, C.; Kushwah, S.; Mangrola, M.H. A Review Article on FDM Process Parameters in 3D Printing for Composite Materials. *Mater. Today Proc.* **2022**, *60*, 2162–2166. [CrossRef]
10. Kristiawan, R.B.; Imaduddin, F.; Ariawan, D.; Ubaidillah; Arifin, Z. A Review on the Fused Deposition Modeling (FDM) 3D Printing: Filament Processing, Materials, and Printing Parameters. *Open Eng.* **2021**, *11*, 639–649. [CrossRef]
11. Borges, M.E.; Hernández, L.; Ruiz-Morales, J.C.; Martín-Zarza, P.F.; Fierro, J.L.G.; Esparza, P. Use of 3D Printing for Biofuel Production: Efficient Catalyst for Sustainable Biodiesel Production from Wastes. *Clean Technol. Environ. Policy* **2017**, *19*, 2113–2127. [CrossRef]
12. Torres, A.; Fuentes, B.; Rodríguez, K.E.; Brito, A.; Díaz, L. Analysis of the Content of Fatty Acid Methyl Esters in Biodiesel by Fourier-Transform Infrared Spectroscopy: Method and Comparison with Gas Chromatography. *J. Am. Oil Chem. Soc.* **2020**, *97*, 651–661. [CrossRef]
13. Díaz, L.; Escalante, D.; Rodríguez, K.E.; Kuzmina, Y.; González, L.A. Response Surface Methodology for Continuous Biodiesel Production from Jatropha Curcas Oil Using Li/Pumice as Catalyst in a Packed-Bed Reactor Assisted with Diethyl Ether as Cosolvent. *Chem. Eng. Process. Process Intensif.* **2022**, *179*, 109065. [CrossRef]
14. *UNE-EN 14103:2020*; Derivados de Aceites y Grasas. Ésteres Metílicos de Ácidos Grasos (FAME). Determinación de Los Contenidos En Éster y En Éster Metílico Del Ácido Linolénico. Asociación Española de Normalización: Madrid, Spain, 2020.
15. Soetaredjo, F.E.; Ayucitra, A.; Ismadji, S.; Maukar, A.L. KOH/Bentonite Catalysts for Transesterification of Palm Oil to Biodiesel. *Appl. Clay Sci.* **2011**, *53*, 341–346. [CrossRef]
16. Zhang, X.; Ma, Q.; Cheng, B.; Wang, J.; Li, J.; Nie, F. Research on KOH/La-Ba-Al_2O_3 Catalysts for Biodiesel Production via Transesterification from Microalgae Oil. *J. Nat. Gas Chem.* **2012**, *21*, 774–779. [CrossRef]
17. Buasri, A.; Chaiyut, N.; Loryuenyong, V.; Rodklum, C.; Chaikwan, T.; Kumphan, N.; Jadee, K.; Klinklom, P.; Wittayarounayut, W. Transesterification of Waste Frying Oil for Synthesizing Biodiesel by KOH Supported on Coconut Shell Activated Carbon in Packed Bed Reactor. *Sci. Asia* **2012**, *38*, 283. [CrossRef]
18. López, D.E.; Goodwin, J.G.; Bruce, D.A.; Furuta, S. Esterification and Transesterification Using Modified-Zirconia Catalysts. *Appl. Catal. A Gen.* **2008**, *339*, 76–83. [CrossRef]
19. Bueno, A.C.; Mayer, M.; Weber, M.; Bechelany, M.; Klotz, M.; Farrusseng, D. Impregnation Protocols on Alumina Beads for Controlling the Preparation of Supported Metal Catalysts. *Catalysts* **2019**, *9*, 577. [CrossRef]
20. Munnik, P.; de Jongh, P.E.; de Jong, K.P. Recent Developments in the Synthesis of Supported Catalysts. *Chem. Rev.* **2015**, *115*, 6687–6718. [CrossRef]
21. *UNE-EN 14214:2020*; Requisitos y Métodos de Ensayo Para Biodiésel (FAME) Para Mo-Tores Diésel. Asociación Española de Normalización: Madrid, Spain, 2020.

22. Wen, G.; Yan, Z.; Smith, M.; Zhang, P.; Wen, B. Kalsilite Based Heterogeneous Catalyst for Biodiesel Production. *Fuel* **2010**, *89*, 2163–2165. [CrossRef]
23. Salim, R.A.; Erwa, I.Y.; Hassan, A.A.; Almaleeh, M.A.; Eldaim, S.O.A.; Ahmed, A.; Yasin, S. Synthesis and Characterization of Li -Zeolite Catalyst for Biodiesel Production from Castor Oil. *Orient. J. Chem.* **2024**, *40*, 1281–1289. [CrossRef]